Eye-Centered Color Adaptation in Global Illumination

A. Gruson[1], M. Ribardière[1] and R. Cozot[1]

[1]IRISA, Université de Rennes 1, France

Figure 1: *Global illumination rendering without Chromatic Adaptation (left), with Chromatic Adpatation (middle), carpet's color comparison (right)*

Abstract

Color adaptation is a well known ability of the human visual system (HVS). Colors are perceived as constant even though the illuminant color changes. Indeed, the perceived color of a diffuse white sheet of paper is still white even though it is illuminated by a single orange tungsten light, whereas it is orange from a physical point of view. Unfortunately global illumination algorithms only focus on the physics aspects of light transport. The ouput of a global illuminantion engine is an image which has to undergo chromatic adaptation to recover the color as perceived by the HVS. In this paper, we propose a new color adaptation method well suited to global illumination. This method estimates the adaptation color by averaging the irradiance color arriving at the eye. Unlike other existing methods, our approach is not limited to the view frustrum, as it considers the illumination from all the scene. Experiments have shown that our method outperforms the state of the art methods.

Categories and Subject Descriptors (according to ACM CCS): I.3.7 [Computer Graphics]: Three-Dimensional Graphics and Realism—Color, shading, shadowing, and texture

1. Introduction

Color adaptation also named color constancy is one of the main ability of the Human Visual System (HVS) [Fai05]. It makes us perceive colors as constant even though the illumination conditions change. For example we perceive the same white color for a white shirt outdoors at midday or indoors under tungsten lights. From a physics point of view, the white shirt color illuminated by the midday sun is quite physically white, but it becomes physically orange under tungsten lights. This shows that the color perception of human being is not only determined by the spectral distribution of light.

Global illumination rendering engines [PH10] physically simulate light transport to compute the pixel colors. But due to chromatic adaptation, these colors are not those that a human perceives. Neumann et al. [NCNS03] had pointed out that global illumination images have to undergo chromatic adaptation to recover the perceived color. The effect of color adptation is demonstrated in Figure 1.

Chromatic adaptation strongly depends on the used adptation color (white balancing). Estimating this adaptation color in case of virtual scenes could appear simple as the geometry, the material appearance as well as the light sources are known data. But, as shown later on, the existing approaches

do not provide convincing results for complex lighting conditions (high color variation of light and material). Designing a method to efficiently estimate the adaptation color still is challenging.

We propose a new method that considers the eye (viewpoint) as a hemispherical sensor arround the eye. The adaptation color is computed as the average irradiance color over this sensor. In this way, flickering artefacts are avoided in case of walkthrough unlike the existing approaches.

The main advantages of our method are:

- the obtained results are faithful to reality,
- temporal coherence in case of animation,
- easy plug-in in existing global illumination renderers.

The paper is structured as follows. Section 2 provides a brief overview on chromatic adaptation, while section 3 reviews the related works. Section 4 provides details on our adaptation color method. Some results are presented in section 5. Finally section 6 concludes our paper.

2. Chromatic Adaptation

In his book [Fai05], Fairchild compares different chromatic adaptation models. Most of the chromatic adaptation models rely on Von Kries' hypothesis which considers that each photoreceptor (L, M, S) adapts linearly independently of each other [VK70]:

$$\begin{bmatrix} L_a \\ M_a \\ S_a \end{bmatrix} = \begin{bmatrix} 1/L_W & 0 & 0 \\ 0 & 1/M_W & 0 \\ 0 & 0 & 1/S_W \end{bmatrix} \begin{bmatrix} L \\ M \\ S \end{bmatrix} \quad (1)$$

where L,M,S are the initial cone responses, L_a,M_a,S_a the adapted cone signals and L_w,M_w,S_w the adaptation color, also called illuminant color or white color.

Some improvements have been brought to the Von Kries transform such as non linear adaptations [BW92, CW95, NTS81, L.91] and degree of adaptation [Bre87, Fai91b, Fai91a]. For example, the chromatic adaptation model [CIE98] modifies the Von Kries transform using an exponential non linearity added to the short wavelength stimuli as well as a parameter D that specifies the degree of adaptation:

$$\begin{cases} R_a = \left[D(1/R_W) + (1-D) \right] R \\ G_a = \left[D(1/G_W) + (1-D) \right] G \\ B_a = \left[D(1/B_W^p) + (1-D) \right] B^p \\ \\ p = (B_W/1.0)^{0.00834} \\ D = F \left[1 - \frac{1}{\left[1 + 2L_A^{1/4} + \frac{L_A^2}{300} \right]} \right] \end{cases} \quad (2)$$

In summary, the chromatic adaptation models provide the perceived color x_a of a stimulus x under given lighting conditions x_W (adaptation color). These models can be expressed as a function of two variables x and x_W:

$$x_a = CAT(x, x_W) \quad (3)$$

Consequently, chromatic adaptation consists of two steps: estimate the adaptation color from the scene or image, then perform the chromatic adaptation transform (See Figure 2). The results of chromatic adaptation strongly depends on the accuracy of the adaptation color.
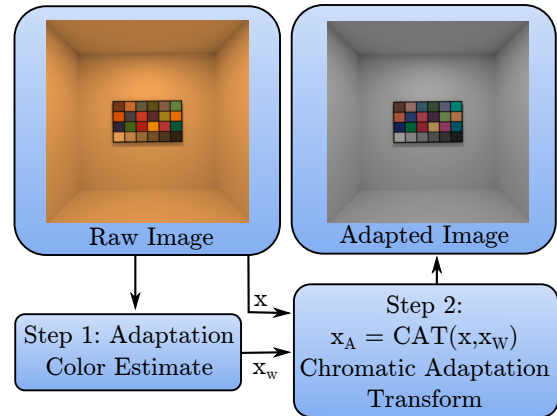

Figure 2: *The 2 steps of the chromatic adaptation process*

3. Related works

In the compter vision field, several methods have beeeen proposed to estimate the adaptation color. They are classified according to three main approaches [TTP08]:

1. physics-based (dichromatric models, maxRGB [Lan77], grey-world [Buc80]),
2. statistical (gamut mapping [FHT06], bayesian [GRB*08]),
3. high level methods (high level visual information) [CFB02, VdWSV07].

A comparison of these methods can be found in [Hor06].

Most of the statistical and high level approaches allow to estimate the adaptation color from a set of given illuminants: artificial lighting (tungsten, fluorescent, halogen, etc.), natural lighting (midday sun, rising sun, sunset, cloudy, etc.). Unfortunately, in the context of global illumination these data are not available.

The Grey-World method [Buc80] assumes that the average reflectance in a scene is achromatic, i.e. grey. Then, the color adaptation is computed as the average color of the whole image.

When the image contains large uniformly colored surfaces, the assumption of a Grey-World fails. That is why Weijer et al. [GGW10] proposed a more robust algorithm called

Grey-Edge. They use the average of the gaussian derivative of the pixel colors to estimate the adaptation color.

The MaxRGB [Lan77], dichromatic [YCK05] and Retinex [LM71, MPS09, MPS10] methods assume that the brightest pixels correspond to specular reflection of the light sources. Thereby the maximum RGB pixel is used as the adaptation color.

In [FT04, GGW10], it is shown that the above adptation methods perform similary. However these methods fail for some test cases such as the one called "world of one reflectance" [RB07]. This test case corresponds to two kinds of scene: (1) a grey world lighted with a colored light and (2) the same world with colored objects lit with a white light. Without chromatic adaptation, the images of the two worlds captured with a camera are the same. However they are actually different when seen by a human viewer.

Color Appearance Model (CAM) [KR09, MFH*02, KJF07] are based on chromatic adaptation. The purpose of the CAM models is to compute the color appearance (brightness, lightness, hue, saturation, chroma and colorfullness) of each pixel of an image. They include a local chromatic adaptation step. For each pixel the adaptation color is computed using either a gaussian low-pass filter [MFH*02, KJF07] or an interpolation between a given achromatic white and the geometric mean of the pixel neighborhood [RPK*12].

To our knowledge, only few authors address the chromatic adaptation problem in the context of global illumination.

Greg Ward et al. [WEV02] assume that most scenes contain a single dominant illuminant. In this case, they use the main illuminant color as the adaptation color. When a scene does not contain any dominant illuminant, this method can not be used.

Neumann et al. [NCNS03] define the adaptation color as the weighted average of the irradiances of the white surfaces. A white surface close to the camera axis is assigned a higher weight. When a scene does not contain any white surface, this method can not be applied. The authors mentioned that their approach provides unnatural results when the white surfaces are lit with different colors.

Wilkie and Weidlich [WW09] propose a method that overcomes the limitations of the above mentioned approaches. Their method is capable of handling complex lightings conditions. It proceeds as follows. First, it uses a global illumination algorithm to compute and store the incident illumination over all the surfaces. Next, the surface BRDFs are replaced by an achromatic reflectance, then multiplyied by the incident illumination to get a new image. The pixels of this image are assigned a weight depending on the associated BRDF. The adaptation color is the weighted average of the pixel colors. The value of the weight is maximum if the pixel corresponds to a white surface. However, this approach suffers from two limitations. First, as their adaptation color estimate depends on the color of the viewed surfaces and

the associated weights, even a small camera displacement can entail high variations of the adaptation color estimate, as detailed later on. This first limitation will be called, from now on, spatio-temporal incoherence. Second, assigning a high weight to white surfaces overestimates their color at the detriment of global illumination.

To sum up, the existing methods suffer from spatio-temporal incoherence because the adaptation color estimate is limited to the field of view. In addition, they provide images that do not look real. The reason is that, when calculating the average color, they (1) assign too high weights to the white surfaces, which favors the color of these surfaces at the detriment of the global illumination color, and (2) assign the same weight to close and faraway objects (to/from the camera).

4. Our color adaptation method

4.1. Generalization of chromatic adaptation

The basic assumption of chromatic adaptation is that an object is perceived as white whatever the illuminant conditions. The physical color of a white point of a diffuse surface is the color of the irradiance at this point. If we generalize the chromatic adaptation assumption to any diffuse surface, then the perceived radiance color $L_a(y)$ of a point y is the intrinsic reflectance $\rho(y)$ of the surface. The physical radiance $L(y) = [L_L, L_M, L_S]$ of a point y of a diffuse surface with a reflectance $\rho(y) = [\rho_L, \rho_M, \rho_S]$ and an irradiance $E(y)$ is given by:

$$L(y) = \frac{1}{\pi} E(y) \rho(y) \qquad (4)$$

where:

$$[E(y)] = \begin{bmatrix} E_L(y) & 0 & 0 \\ 0 & E_M(y) & 0 \\ 0 & 0 & E_S(y) \end{bmatrix} \qquad (5)$$

Equation 1 can be rewritten as:

$$L_a(y) = \rho(y) = \frac{1}{\pi} \begin{bmatrix} 1/L_W & 0 & 0 \\ 0 & 1/M_W & 0 \\ 0 & 0 & 1/S_W \end{bmatrix} [E(y)] \rho(y) \qquad (6)$$

Then, the adaptatation radiance $x_W(y)$ has the same color as the irradiance ones:

$$x_W(y) = \frac{1}{\pi} \begin{bmatrix} E_L(y) \\ E_M(y) \\ E_S(y) \end{bmatrix} \qquad (7)$$

4.2. Eye-centered estimate of the adaptation color

As a single global adaptation color is required for the whole image, the adaptation color is usually computed as the weighted average irradiance ([NCNS03]) or radiance

([WW09]) of the white surfaces within the field of view. In our opinion, the main issues of existing methods stem from the weighting average operation and from the space from which is computed the average values (view frustum or all the 3D space containing the camera). First, the averaging operation assigns a higher weight to the white surfaces. Consequently, the average value overestimates the direct lighting on these white surfaces, which underestimates the indirect lighting color. For example if the scene contains a red spotlight that only lights the only white object within the scene, then the direct lighting due to the red spotlight is overestimated, which makes the adapted image look unnatural (Figure 9). Equation 7 shows that there is no reason to assign a higher weight to the color of white surfaces. Second the previous methods do not take into account the distance to the surfaces from the camera when assigning weights since they assign them the same weight. Third, performing an averaging operation only for surfaces lying in the field of view, is not sufficient. Indeed, a small displacement of the camera can result in a high change in the adaptation color. This happens especially when a white surface enters or leaves the field of view.

According to Von Kries hypothesis [VK70] that considers that the photoreceptors are adapted independently of one another, we assume that the adaptation color is the lighting color at the eye location as everyday experience shows that the chromatic adaptation is sensitive to the observer position rather than to the direction he looks at. When the observer is in a room, even tough he sees the illuminant color of another room, he discounts only the illuminant color of the room in which he is located. In other words, the adaptation color depends only on the illuminant color of the room containing the observer.

We also make the assumption that all the directions of lighting arriving at the observer (view angle of 180 degrees) contribute uniformly to its perceived radiance. This means that the chromatic adaptation phenomenon would be sensitive to lighting even when coming from outside the field of view of the camera. This can be explained by the fact that the human eye has an approximately hemispherical field of vision.

Then the chromatic adaptation phenomenon can be modeled by a hemispherical sensor located around the eye. This sensor has an isotropic sensitivity and measures the average color of light arriving at its surface. From a mathematical point of view, it means that the adaptation color x_W^{eye} is the average value of the irradiance colors on a virtual hemisphere located at the eye position and aligned with the gaze direction (Fig. 3):
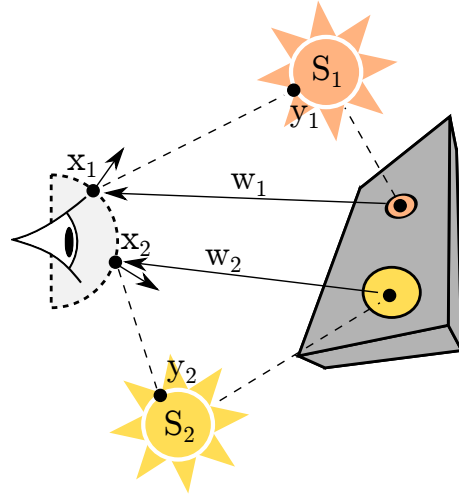
$$x_W^{eye} = \frac{1}{2\pi r^2} \int_{S_\Omega} E(x)dx \qquad (8)$$

where $E(x)$ is the irradiance at a point x on the hemisphere S_Ω of radius r.

The irradiance $E(x)$ is computed as:

$$E(x) = \int_\Omega L_i(x,\omega_i)cos(n_x,\omega_i)d\omega_i \qquad (9)$$

where $L_i(x,\omega_i)$ is the incident luminance of direction direction ω_i at point x, and n_x the normal vector at x. Our new

Figure 3: *Irradiance color average on virtual hemisphere as color adaptation (hemispherical sensor)*

approach has the following main characteristics:

1. the adaptation color is based on the average irradiance at the eye location rather than on the radiance colors in the field of view, more importance is then given to objects close to the eye,
2. the adaptation color does not focus on the irradiance or radiance color of white surfaces, consequently it does not overestimate local lighting,
3. the adaptation color estimate is not limited to the field of view, it is then more robust to camera displacements.

The rendering engine computes the average irradiance color over the virtual hemisphere (Fig. 4), then the color adaptation transform (CAT) is applied to recover the perceived colors. We use the CIE linear chromatic adaptation transform, called CAT02 [MFH*02], to perform the chromatic adaption:

$$\begin{bmatrix} X_a \\ Y_a \\ Z_a \end{bmatrix} = M_{02}^{-1} \begin{bmatrix} R_a \\ G_a \\ B_a \end{bmatrix}, \quad \begin{bmatrix} R \\ G \\ B \end{bmatrix} = M_{02} \begin{bmatrix} X \\ Y \\ Z \end{bmatrix} \qquad (10)$$

$$\begin{aligned} R_a &= \left(\frac{R_O}{R_W^{eye}}D + (1-D)\right)R \\ G_a &= \left(\frac{G_O}{G_W^{eye}}D + (1-D)\right)G \\ B_a &= \left(\frac{B_O}{B_W^{eye}}D + (1-D)\right)B \end{aligned} \qquad (11)$$

where $x_a = [X_a, Y_a, Z_a]$ is the adapted color, $[R_0, G_0, B_0]$
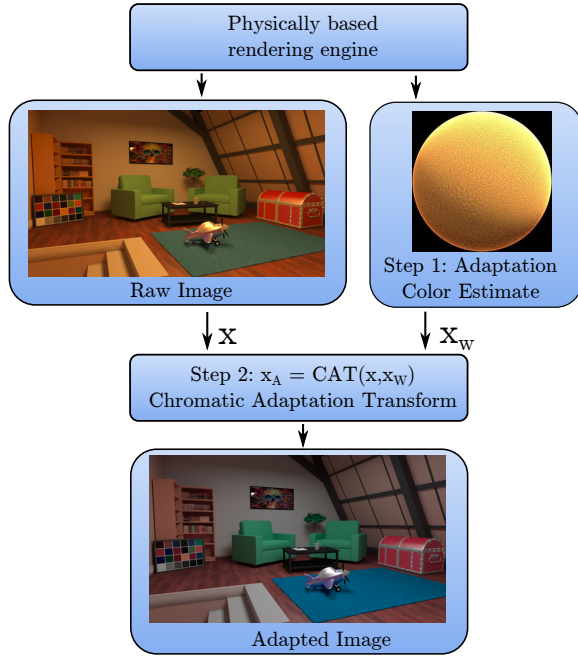
Figure 4: *Architecture overview of our chromatic adaptation process*

the white reference illuminant (D_{65}), $\left[R_W^{eye}, G_W^{eye}, B_W^{eye}\right]$ our adaptation color, D is the degree of adaptation and M_{02} the color space transform matrix used in CAT02.

In our current implementation, we use the Mitsuba physically based renderer [Jak10] and its path tracing integrator. In order to estimate the average irradiance over the hemisphere (Eq. 8), we split the radiance into direct and indirect components to get $L_i(x, \omega_i) = L_e(x, \omega_i) + L_{ind}(x, \omega_i)$, which leads to:

$$x_W^{eye} = \frac{1}{2\pi r_{S_\Omega}^2}\left(\phi_{direct} + \phi_{ind}\right) \qquad (12)$$

with:

$$\phi_{direct} = \int_{S_\Omega}\int_S L_e(y \to x)G(x \leftrightarrow y)dA(y)dA(x) \qquad (13)$$

$$\phi_{ind} = \int_{S_\Omega}\int_H L_{ind}(x, \omega_i)cos(n_{x_i}, \omega_i)d\omega_i dA(x) \qquad (14)$$

where S is all the surfaces comprising the scene. For direct lighting we use a simple sampling method by taking a point y_i on the light source with the probability $P_a(y_i)$ and compute its contribution:

$$\phi_{direct} = \frac{1}{N}\sum_{i=1}^{N}\frac{L_e(y_i \to x_i)G(y_i \leftrightarrow x_i)V(y_i \leftrightarrow x_i)}{P_a(y_i)P_a(x_i)} \qquad (15)$$

where x_i is a sample on the hemisphere with the probability $P_a(x_i)$, $L_e(y_i \to x_i)$ the emitted radiance from y_i to x_i, $G(y_i \leftrightarrow x_i)$ the geometry factor and $V(y_i \leftrightarrow x_i)$ the visiblity term.

For indirect lighting computation, we can use a well known stochastic ray tracing technique by taking a point on the hemisphere x_i and a random incident direction ω_i with the probability $P_\sigma(x_i, \omega_i)$:

$$\phi_{ind} = \frac{1}{N}\sum_{i=1}^{N}\frac{L_{path}(x_i, \omega_i)cos(n_{x_i}, \omega_i)}{P_a(x_i)P_\sigma(x_i, \omega_i)} \qquad (16)$$

where L_{path} is a radiance computed by a path tracer using multiples bounces.

Moreover, the evaluation of the estimators (eq. 15 and 16) is time consuming and depend on the number of samples N. However, the cost of these evaluations is negligible when considering the cost of the global illumination computation for the whole image. Indeed, in our experiments, we used 0.1% of the total samples count used to render an image.

Our adaptation color operation can also be done using commercial global illumination engines which are not open source. In this case, we proceed the following way : (1) we render the 3D scene in which we add a little diffuse white hemisphere located at the camera position just ahead the front clipping plane, (2) we add on orthographic camera looking at the hemisphere, (3) we render an image of the hemisphere and compute the average radiance L_{av} over the hemisphere, (4) finally the average irradiance (πL_{av}) color gives the adaptation color. This implementation works well because adding a small hemisphere does not change significantly the rendering solution.

Our eye-centered estimate of color adaptation gives the expected results (see section 5) in the classic test cases, these results are similar to those obtained with the Wilkie and Weidlich's method. But for scenes with complex lighting our approach provides images that look more natural compared to [WW09].

5. Results

First, we used the benchmark cases listed in [WW09] for color adaptation: direct lighting, world of one reflectance and indirect lighting. In these test cases there is only one illuminant and their corresponding results are known (section 5.1). In addition, we added more complex test cases (section 5.2). By complexity we mean: high irradiance color variations (when the camera moves from one room to another, spotlight), several illuminants with different colors. In these latter cases, the expected results are not avalaible. Therefore we can only discuss if the adapted image looks natural. Finally we also show results for walkthrough (section 5.3).

For each case, we provide three images. The first one, called *raw* image, does not undergo chromatic adaptation, while the two other ones result from chromatic adaptation using our approach and the method presented in [WW09]. As Wilkie's method is the most recent and most efficient for color adaptation in the context of global illumination, we compare it to our approach through different test cases. In

Wilkie's method, the parameter *w* which controls the influence of the "white object information" is set to the value 2 (optimal value according to the authors). In our method, the degree of adaptation *D* (Eq. 11) is set to 1 in order to compute a complete adaptation as in Wilkie's method. From now on, Wilkie's method will be called *WCAM*, which stands for *W*ilkie *C*olor *A*daptation *M*ethod.

5.1. Standard tests cases

The first standard test case consists of a white Cornell box with an orange light source (see Figure 5). In this case Wilkie's method and ours provide the same adaptation color which corresponds to the expected one.

The second test case is the worlds of one reflectance: White World-Orange Light and Orange World-White Light. Wilkie's method and ours give the expected adptation colors. The actual object reflectances are recovered in both cases (Figure 6 and 7).

The third case consists of a Cornell box with a diffuse green floor (see Figure 8). The light source color is white. Due to indirect illumination, a green lighting component is clearly noticeable on the raw image (see Figure 8, left image). *WCAM* overestimates this green component, hence the facing wall above the color checker appears slightly purple: (hue=292, saturation=5%). With our adaptation color, the same pixel is still a litle bit green: (hue=132, saturation=2%), which looks more natural.

As in all the above test cases, the illuminant color is almost uniform within the scene, *WCAM* and our method provide the same color adaptation. Indeed, as the illuminant color is the same from all the object's scene, computing the adaptation color within either the field of view or a 180 degree frustum lead to the same result. Even for a moderate variation of irradiance color in the scene, our method outperforms *WCAM*, as seen in Figure 8.

5.2. Complex tests cases

The first complex test case consists of a room containing a white Buddha statue lit by a red lightspot and a main white light source located on the ceiling (see figure 9). *WCAM* computes a red adaptation color because the white statue is partially lit by a red spotlight. Consequently, after chromatic adaptation, the part of the statue lit by the spotlight gets a white color while the part takes a blue color, which looks unnatural. Instead, our method provides a result that looks more natural.

The second test case consists of a scene made of two rooms (Figure 10). The first one is lit with four orange light sources while the second is lit with four blue ones. We computed three images (Figure 12). In the first one (red view frustum), the second room is not visible. In the second image (green view frustum), both rooms are visible. In the third


Figure 9: *Chromatic adaptation results when a red spotlight partially lits a white statue, raw image (up), using WCAM (middle), using our adaptation color (bottom)*

image (blue view frustum), only the second room is visible while the camera lies in the first room.

In this case, *WCAM* computes three different adaptation colors because it considers only the visible objects to compute the adaptation color. Regarding our method, it also computes three adaptation colors which are very close to each other (Figure 11). This can be explained by the fact that our approach is sensitive to where the camera is located rather than the visible surfaces. These results shows that lacks spatio-temporal coherency.

5.3. Sequence tests cases

We tested our algorithm on video sequences to demonstrate its ability to meet the constraint of spatio-temporal coherency. The video sequence shown in this paper is a walkthrough into a scene composed of three rooms with different illuminant colors (Figure 13). The camera starts in a room lit
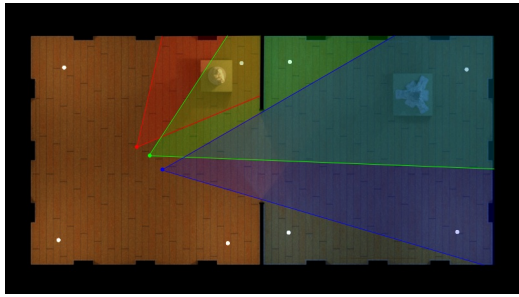
Figure 10: *Map of a 2 room scene and 3 view frustrums (red, blue, green)*
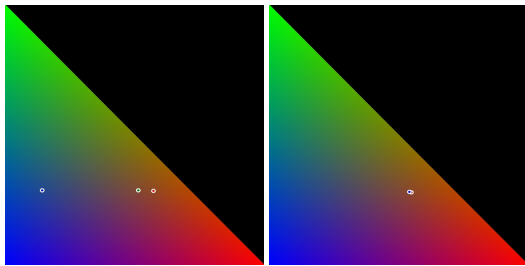
Figure 11: *Chromaticity diagram for RGB color space. The small circles represent the adaptation colors for the 3 frustums of Figure 10, obtained with WCAM (left) and our method (right). The circle color (red, green, blue) corresponds to the frustum*

Figure 13: *Map of a 3 room scene and camera trajectory*

Figure 14: *Adaptation colors for each frame of the video sequence with WCAM (bottom), with our method (up)*

with a white light, then goes through another room lit with an orange light,to finally reach a room lit with a blue light.

Figure 14 shows the adaptation color for each frame of the sequence. Unlike *WCAM*, our method provides a smooth variation of the adaptation color. Note that the *WCAM* results in a sudden change of the adaptation colors, especially at the beginning of the sequence ((1) insert box in figure 14). In addition, the *WCAM* adapts too early to the illuminant color of the third room ((2) green insert in figure 14)
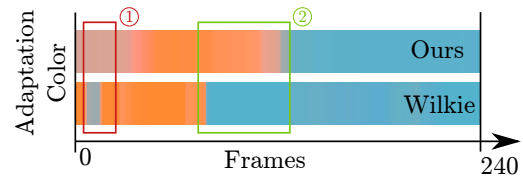
The sudden change in the adapation color in *WCAM* occurs between frames 5 and 10 (Figure 15). The rendered image does not change so much between these frames. Only the specular reflection of one light source on the bench (red insert in Figure 15, middle) changes significantly, which highly changes the adaptation color. The reason is that *WCAM* adapts mostly to this specular reflection while our method adapts to the average irradiance color over the hemispherical sensor as shown in Figure 15(rightmost image). The video sequence is provided as an additionnal material.

6. Conclusion

We have proposed a simple, accurate and spatio-temporally coherent method to automatically estimate the adaptation

color for chromatic adaptation in the context of global illumination. Our adaptation color is computed as the average of irradiance color over a virtual hemispherical sensor centered at the camera location and aligned with the camera axis. First, we have demonstrated that our algorithm outperforms the state of the art methods especially when the illuminant color varies in a scene. Second, as our mehod is spatio-temporally coherent it can be used in video sequences. Third, it can be easily implemented using an open or closed source rendering engine.

Future work would extend the use of hemispherical sensor to tone mapping (also called light adptation) video sequences, thanks to the spatio-temporal coherence property of the hemispherical sensor. Another research avenue is to propose an alternative (other norms) to just averaging the irradiance color to compute the adaptation color.

References

[Bre87] BRENENAM E. J.: Corresponding chromaticities for different states of adaptation to complex visual fields. *Journal of the Optical Society of America A 4* (1987), 1115–1129. 2

[Buc80] BUCHSBAUM G.: A spatial processor model for object

colour perception. *Journal of the Franklin Institute 310* (1980). 2

[BW92]   BRAINARD D., WANDELL B.: asymmetric color matching : how color appearance depends on the illuminant. *Journal of the Optical Society of America A 9* (1992), 1433–1448. 2

[CFB02]   CARDEI V., FUNT B., BARNARD K.: Estimating the scene illumination chromaticity using a neural network. *Journal of the Optical Society of America 19*, 12 (2002). 2

[CIE98]   CIE: *The CIE 1997 Interim Colour Appearance Model*. John Wiley and sons, Ltd, 1998. 2

[CW95]   CHICHILNISKY E. J., WANDELL B. A.: Photoreceptor sensitivity changes explain color appearance shifts induced by large uniform backgrounds in dichoptic matching. *Vision Research 53* (1995), 239–254. 2

[Fai91a]   FAIRCHILD M. D.: Formulation and testing of an incomplete-chromatic-adaptation model. *Color Research Application 16* (1991), 243–250. 2

[Fai91b]   FAIRCHILD M. D.: A model of incomplete chromatic adaptation. In *the 22nd Session of the CIE* (1991), CIE, pp. 33–34. 2

[Fai05]   FAIRCHILD M. D.: *Color Appearance Model, Second edition*. John Wiley and sons, Ltd, 2005. 1, 2

[FHT06]   FINLAYSON G. D., HORDLEY S. D., TASTL I.: Gamut constrained illuminant estimation. *Int. J. Comput. Vision 67*, 1 (2006), 93–109. doi:http://dx.doi.org/10.1007/s11263-006-4100-z. 2

[FT04]   FINLAYSON G. D., TREZZI E.: Shades of Gray and Colour Constancy. In *Color Imaging Conference* (2004), pp. 37–41. 3

[GGW10]   GIJSENIJ A., GEVERS T., WEIJER J.: Generalized gamut mapping using image derivative structures for color constancy. *Int. J. Comput. Vision 86*, 2-3 (2010), 127–139. doi:http://dx.doi.org/10.1007/s11263-008-0171-3. 2, 3

[GRB*08]   GEHLER P., ROTHER C., BLAKE A., MINKA T., SHARP T.: Bayesian color constancy revisited. pp. 1–8. doi:10.1109/CVPR.2008.4587765. 2

[Hor06]   HORDLEY S. D.: Scene illuminant estimation: past, present, and future. *Color Research and Application 31*, 4 (2006), 303–314. 2

[Jak10]   JAKOB W.: Mitsuba renderer, 2010. http://www.mitsuba-renderer.org. 5

[KJF07]   KUANG J., JOHNSON G. M., FAIRCHILD M. D.: icam06: A refined image appearance model for hdr image rendering. *Journal of Visual Communication* (2007). 3

[KR09]   KUNKEL T., REINHARD E.: A neurophysiology-inspired steady-state color appearance model. *Journal of the Optical Society of America A 26*, 4 (April 2009), 776–782. URL: http://www.cs.bris.ac.uk/Publications/Papers/2001006.pdf. 3

[L.91]   L. G. S.: Model for color vision and light adaptation. *Journal of the Optical Society of America A 8* (1991), 976–993. 2

[Lan77]   LAND E. H.: The retinex theory of color vision. *Scientiþc American 237*, 6 (1977), 108–120. 2, 3

[LM71]   LAND E. H., MCCANN J. J.: Lightness and retinex theory. *J. Opt. Soc. Am. 61*, 1 (Jan 1971), 1–11. URL: http://www.opticsinfobase.org/abstract.cfm?URI=josa-61-1-1, doi:10.1364/JOSA.61.000001. 3

[MFH*02]   MORONE Y. N., FAIRCHILD M. D., HUNT R. W. G., LI C., LOU M. R., NEWMAN T.: The ciecam02 color appearance model. In *In Color Imaging Conference (2002), IS&T* (2002), Society for Imaging Science and Technology, pp. 23–27. 3, 4

[MPS09]   MOREL J.-M., PETRO A. B., SBERT C.: Fast implementation of color constancy algorithms. In *Proc. SPIE 7241, Color Imaging XIV: Displaying, Processing, Hardcopy, and Applications, 724106 (January 19, 2009)* (2009). doi:http://dx.doi.org/10.1117/12.805474. 3

[MPS10]   MOREL J. M., PETRO A. B., SBERT C.: A pde formalization of retinex theory. *Trans. Img. Proc. 19*, 11 (Nov. 2010), 2825–2837. URL: http://dx.doi.org/10.1109/TIP.2010.2049239, doi:10.1109/TIP.2010.2049239. 3

[NCNS03]   NEUMANN L., CASTRO F., NEUMANN A., SBERT M.: Color appearance in multispectral radiosity. In *Proceedings on the 2nd Hungarian Computergraphics and Geometry Conference* (2003), L. Szirmay-Kalos G. R., (Ed.), pp. 183–194. URL: http://www.cg.tuwien.ac.at/research/publications/2003/neumann-2003-color/. 1, 3

[NTS81]   NAYATANI Y., TAKAHAMA K., SOBAGAKI H.: Formulation of anonlinear model of chromatic adaptation. *Color Research Application 6* (1981), 161–171. 2

[PH10]   PHARR M., HUMPHREYS G.: *Physically Based Rendering, Second Edition: From Theory To Implementation*, 2nd ed. Morgan Kaufmann Publishers Inc., San Francisco, CA, USA, 2010. 1

[RB07]   RUPPERTSBERG A. I., BLOJ M.: Reflecting on a room of one reflectance. *Journal of Vision 7*, 13 (2007), –. URL: http://www.journalofvision.org/content/7/13/12.abstract, arXiv:http://www.journalofvision.org/content/7/13/12.full.pdf+html, doi:10.1167/7.13.12. 3

[RPK*12]   REINHARD E., POULI T., KUNKEL T., LONG B., BALLESTAD A., DAMBERG G.: Calibrated image appearance reproduction. *ACM Trans. Graph. 31*, 6 (Nov. 2012), 201:1–201:11. URL: http://doi.acm.org/10.1145/2366145.2366220, doi:10.1145/2366145.2366220. 3

[TTP08]   TREMEAU A., TOMINAGA S., PLATANIOTIS K. N.: Color in image and video processing: Most recent trends and future research directions. *EURASIP Journal on Image and Video Processing 2008* (2008). 2

[VdWSV07]   VAN DE WEIJER J., SCHMID C., VERBEEK J.: Using high-level visual information for color constancy. In *IEEE Conference on Computer Vision (ICCV)* (2007). 2

[VK70]   VON KRIES J.: *Chromatic adaptation*. MIT Press, 1970, pp. 109–119. 2, 4

[WEV02]   WARD G., EYDELBERG-VILESHIN E.: Picture perfect rgb rendering using spectral prefiltering and sharp color primaries. In *EGRW '02: Proceedings of the 13th Eurographics workshop on Rendering* (Aire-la-Ville, Switzerland, Switzerland, 2002), Eurographics Association, pp. 117–124. 3

[WW09]   WILKIE A., WEIDLICH A.: A robust illumination estimate for chromatic adaptation in rendered images. In *Eurographics Symposium on Rendering 2009* (2009). 3, 4, 5

[YCK05]   YOON K.-J., CHOFI Y. J., KWEON I.-S.: Dichromatic-based color constancy using dichromatic slope and dichromatic line space. In *Image Processing, 2005. ICIP 2005. IEEE International Conference on* (2005), vol. 3, pp. III–960–3. doi:10.1109/ICIP.2005.1530553. 3
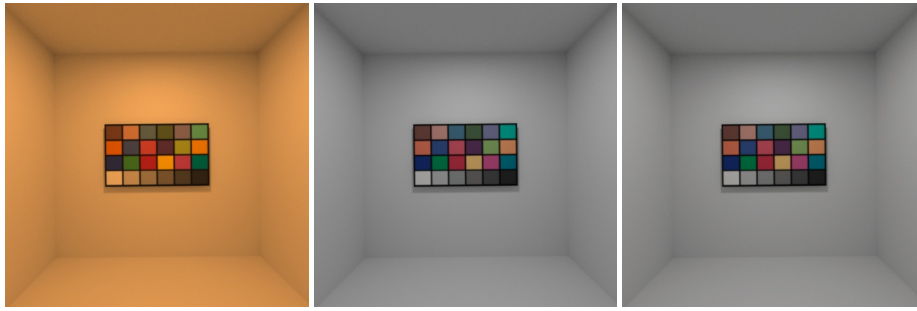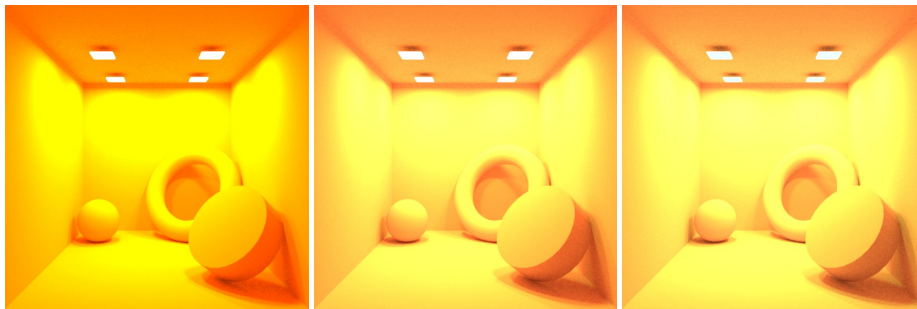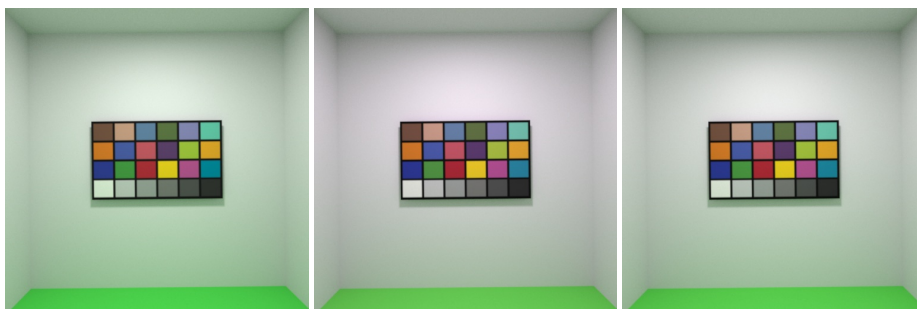
Figure 5: *Color light source*
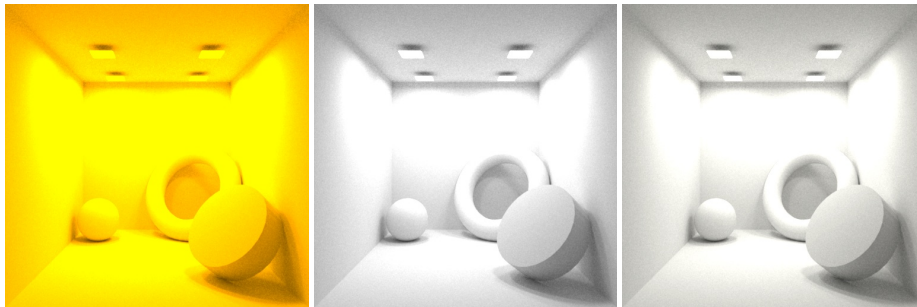
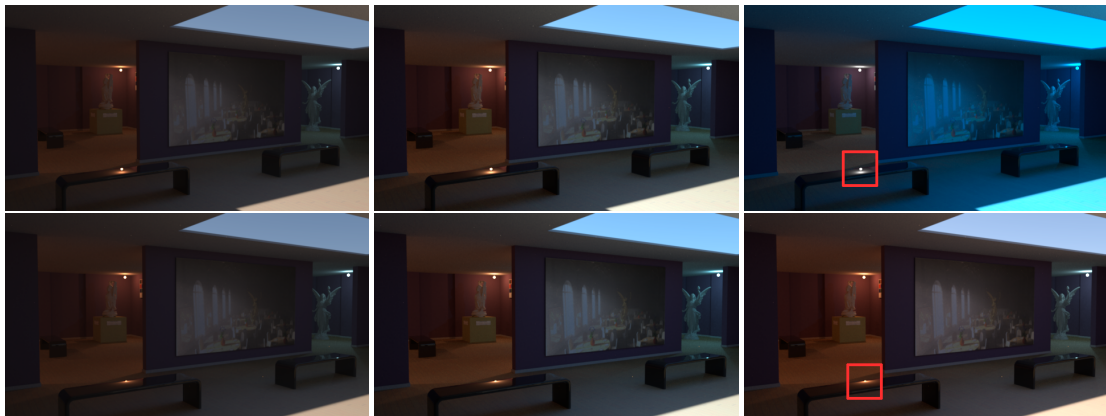**Figure 6:** *White World - Orange Light*

Figure 7: *Orange World - White Light*

Figure 8: *White Light with colored indirect illumination lighting component*

raw image (up), using *WCAM* (middle), using our adaptation color (bottom)

Figure 12: *Spatial coherency of the adaptation color estimate in the case of 2 room scene. raw image(left), using WCAM (middle), using our method (right)*

Figure 15: *Video sequence. Spatio-temporel coherency issue between frame 5 (up) and 10 (bottom), raw image (left), ours (middle), specular highlight changing the estimate (right)*